Supporting information for

A New Tri-nuclear Cu-carbonate Cluster Utilizing CO_2 as C1-Building Block-Reactive Intermediates, Probable Mechanism, EPR and Magnetic Studies

Biswanath Das,*[†] Mohan Bhadbhade,[‡] Anders Thapper,[±] Chris D Ling,[§] Stephen B Colbran*[†]

[†]School of Chemistry, University of New South Wales, Sydney 2052, Australia
[‡]Mark Wainwright Analytical Centre, University of New South Wales, Sydney 2052, Australia
[±]Department of Chemistry – Ångström Laboratory, Uppsala University, SE-75120, Uppsala, Sweden
[§]School of Chemistry, The University of Sydney, Sydney 2006, Australia

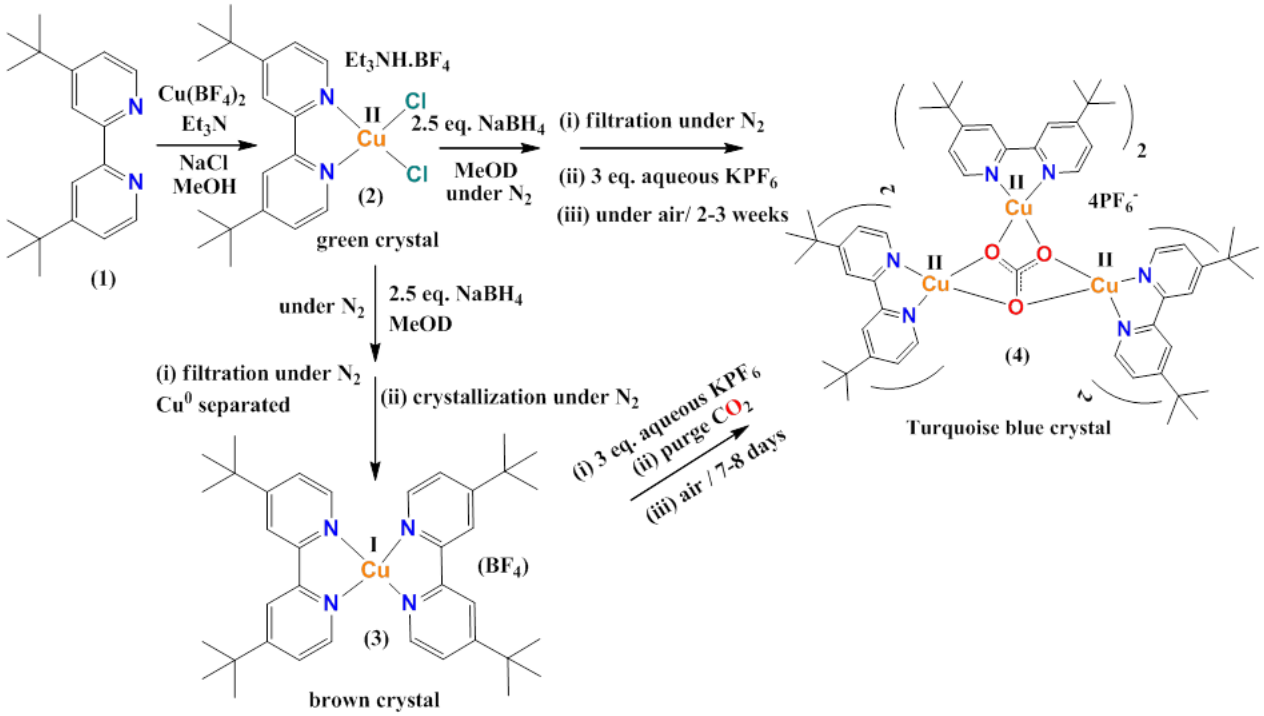

Scheme S1. Detailed schematic representation of the reaction pathway.

Table S1. Crystal data and refinement details for **2**, **3** and **4.**

compound	**2** [CCDC 1880852]	**3**[CCDC 1880853]	**4**[CCDC 1880854]
empirical formula	$C_{24}H_{40}Cl_2N_3B_1F_4Cu_1$	$C_{18}H_{24}N_2B_{0.5}F_2Cu_{0.5}$	$C_{36.33}H_{48}N_4OF_8Cu_1P_{1.33}$
formula weight	591.84	343.57	813.62
crystal size [mm³]	0.226×0.044×0.022	0.326×0.135×0.045	0.114× 0.107× 0.036
crystal system	triclinic	trigonal	trigonal
space group	*P*–1	*P3221*	*R3*
a [Å]	7.4731(5)	11.2232(15)	19.4230(19)
b [Å]	13.2115(10)	11.2232(15)	19.4230(19)
c [Å]	14.9811(11)	27.924(4)	29.434(3)
α [°]	86.824(4)	90.00	90.00
β [°]	81.552(4)	90.00	90.00
γ [°]	81.251(4)	120.00	120.00
V [Å³]	1445.20(18)	3046.0(9)	9616(2)
Z	2	6	9
ρ [g/cm³]	1.360	1.124	1.264
F(000)	618	1086	3807
μ [mm^{-1}]	0.984	0.583	0.627
T_{min} / T_{max}	0.6772/ 0.7455	0.6189/ 0.7456	0.6255/0.7456
θ-range [°]	2.751- 27.062	2.188- 24.987	2.789– 27.062
hkl-range	±9, ±16, ±19	-13 +12, -13 +13, -32 33	±23, ±23, -29 34
measured refl.	8117	6850	2663
unique refl. [R_{int}]	30697 [0.0595]	19079 [0.0425]	23382 [0.1113]
observed refl. ($I > 2\sigma(I)$)	4822	3228	3786
data / restraints / param.	6317 / 149 / 433	3579 / 19 / 218	6937/ 330/ 488
goodness-of-fit (F^2)	1.035	1.097	1.025
*R*1, *wR*2 ($I > 2\sigma(I)$)	0.0424, 0.1096	0.0787, 0.2163	0.0812, 0.2111
*R*1, *wR*2 (all data)	0.0619, 0.1222	0.0857, 0.2253	0.1592, 0.2586
resid. el. dens. [e/Å³]	-0.438/ 0.862	-1.147/ 1.060	-1.068/0.687

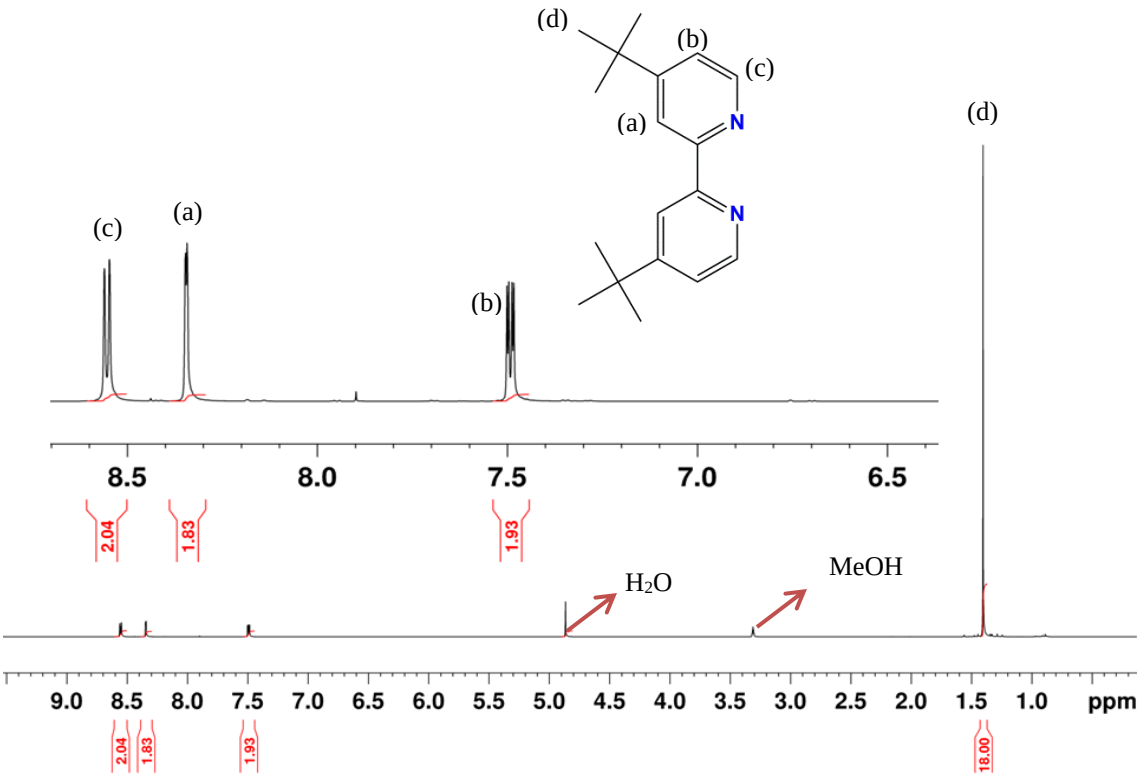

Figure S1. 400 MHz NMR spectra of a 0.025M solution of **1** in MeOD. Inset shows magnified spectra of the range 6 ppm to 8.7 ppm.

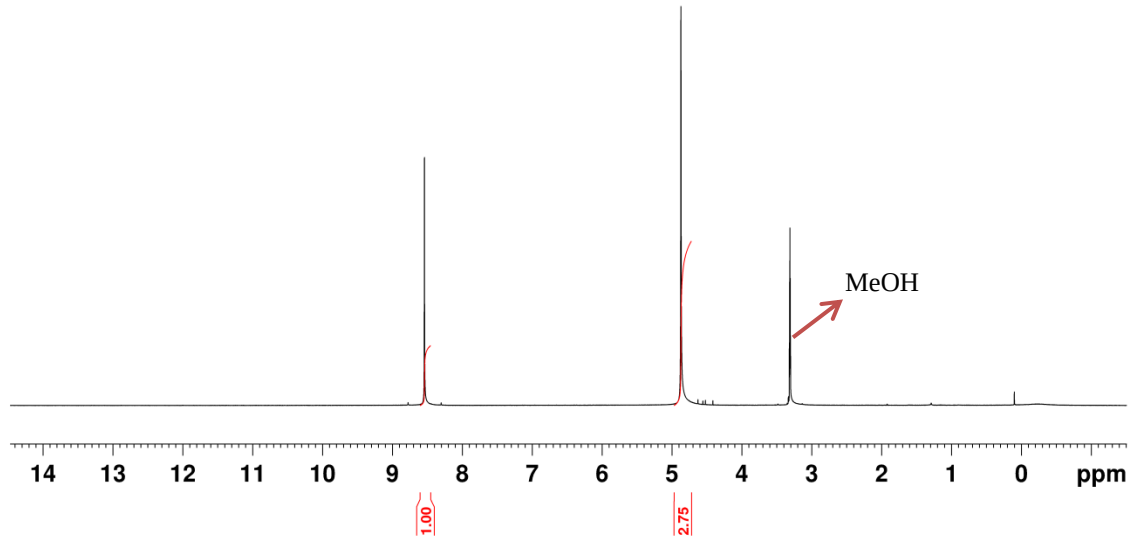

Figure S2. 400 MHz NMR spectra of a 0.05M solution of $NaBH_4$ in MeOD after purging CO_2 for 3 minutes; the formation of $Na[H_3B(OCHO)]$.[1, 2]

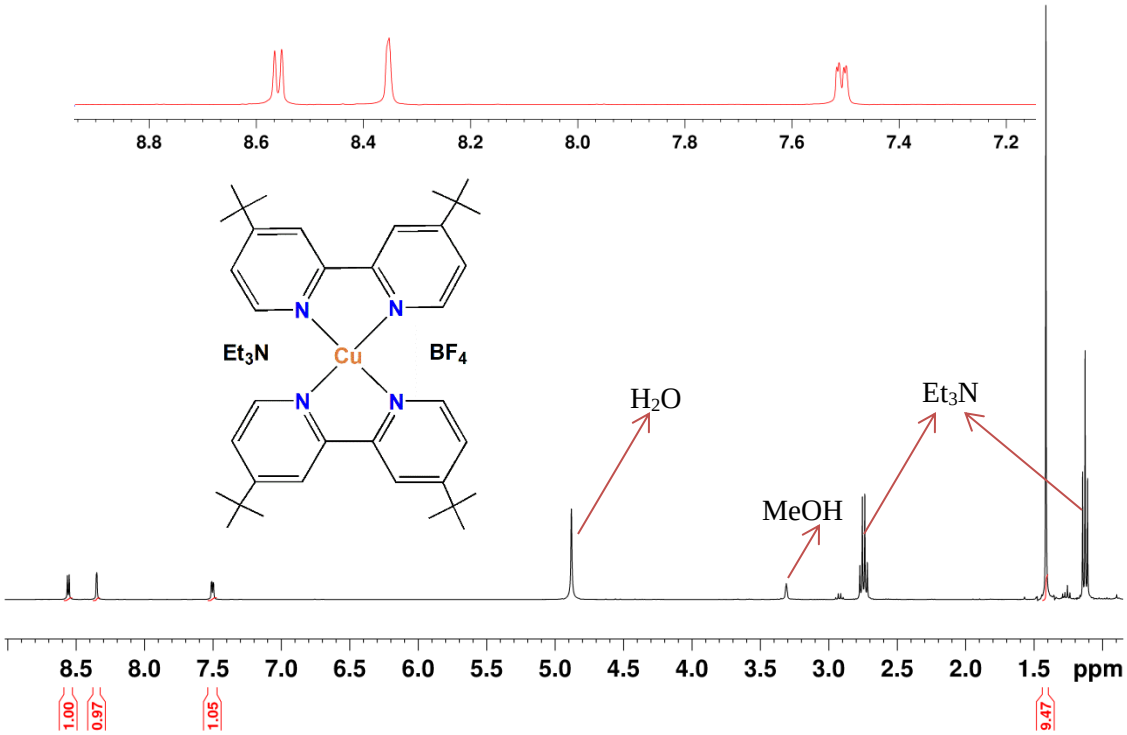

Figure S3. 400 MHz NMR spectra of the in-situ generated MeOD solution of **3 +** remaining excess of Et_3N & $NaBH_4$. Inset shows magnified spectra of the range 7.2 ppm to 8.9 ppm.

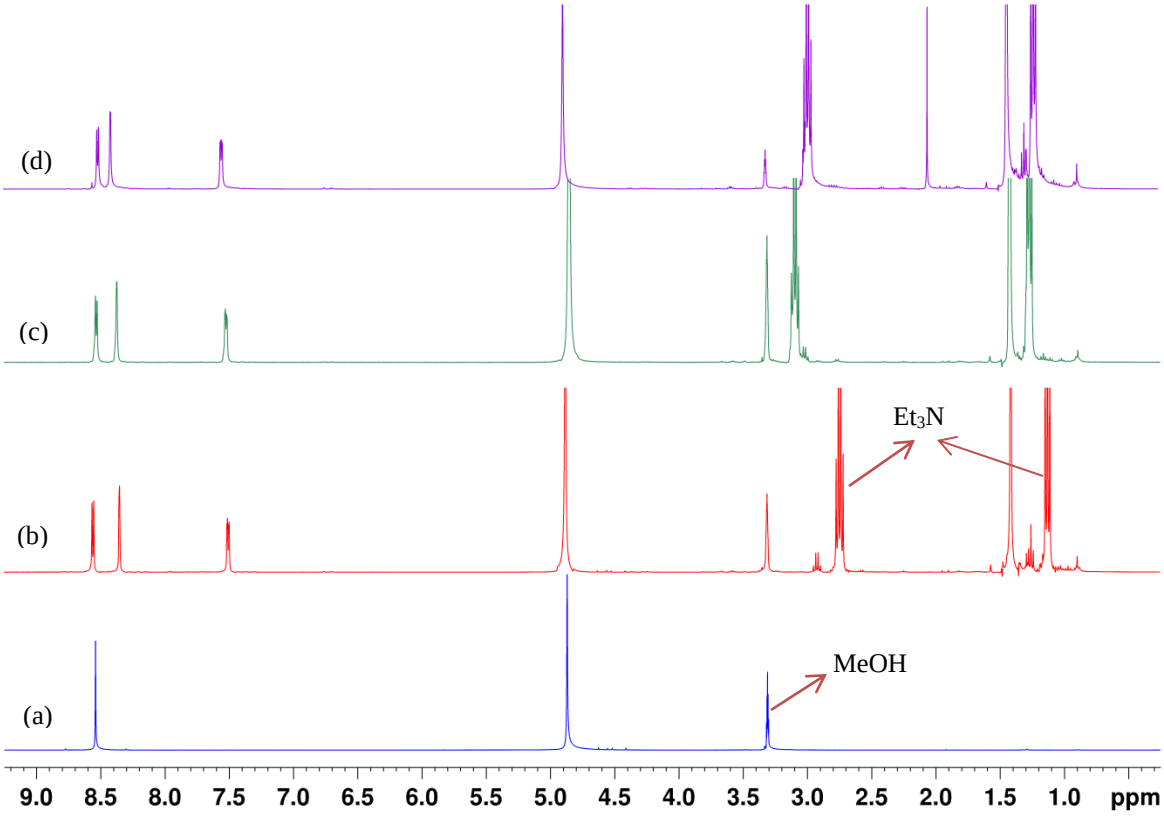

Figure S4. 400 MHz NMR spectra of (a) a 0.05M solution of $NaBH_4$ in MeOD after purging CO_2 for 3 minutes, (b) in-situ generated MeOD solution of **3 +** remaining excess of Et_3N & $NaBH_4$, (c) b + 1atm CO_2 after 24 h and (d) b + 1atm CO_2 after 48 h. The changes in the chemical shift values of the aromatic hydrogens with time are depicted in figure S5.

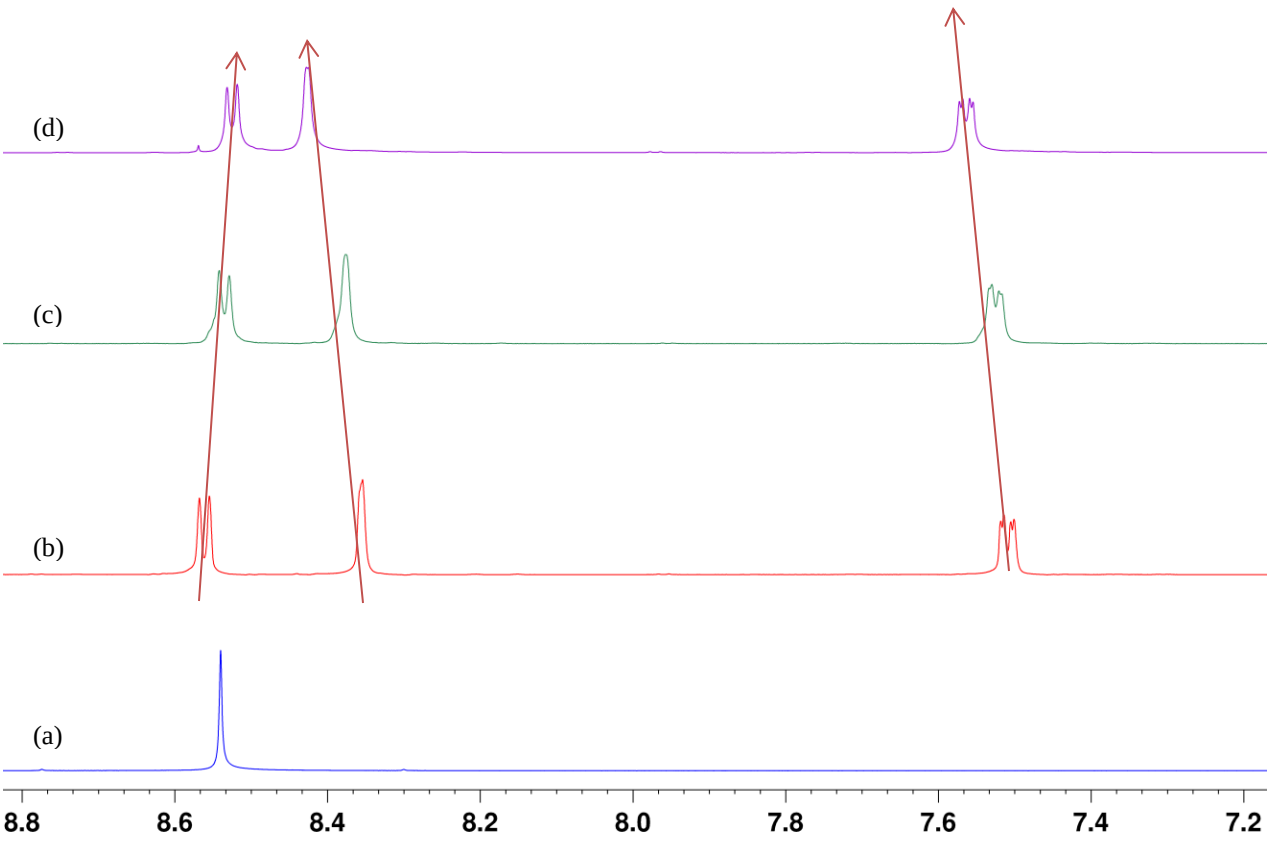

Figure S5. Magnified depiction of figure 4s of the range 7.2 ppm to 8.8 ppm, showing change over a period of 48 h.

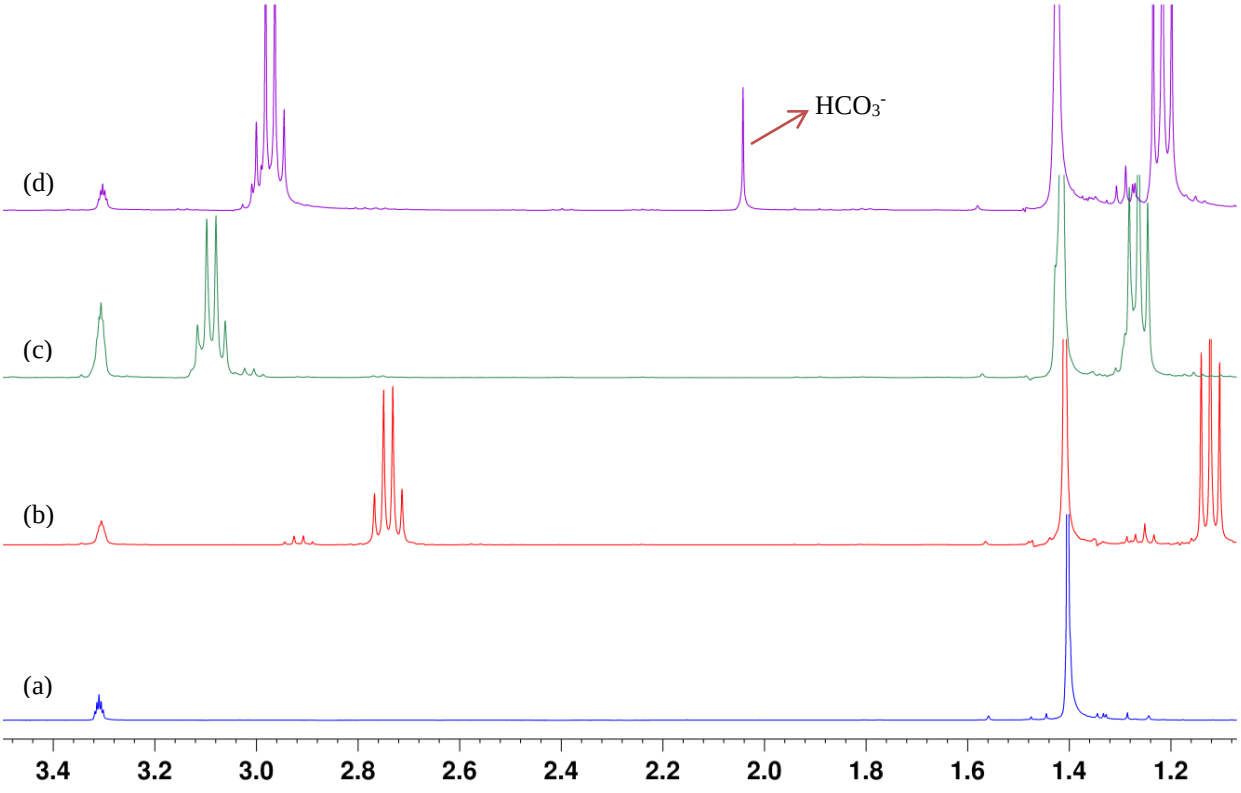

Figure S6. Magnified depiction of figure 4s of the range 1.1 ppm to 3.5 ppm, showing change in the structure over a period of 48 h.[3, 4]

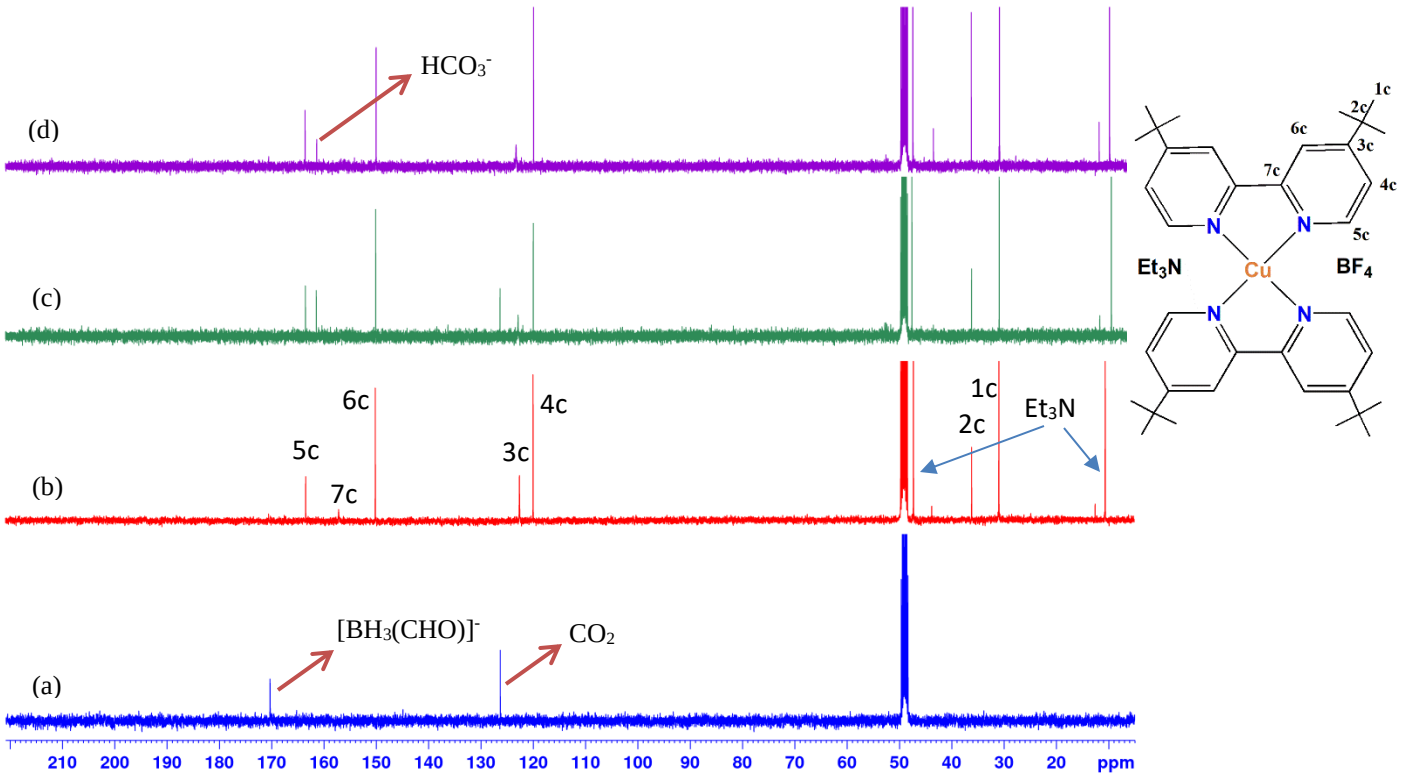

Figure S7. 100.6 MHz ^{13}CNMR spectra of (a) a 0.05M solution of $NaBH_4$ in MeOD after purging CO_2 for 3 minutes, (b) in-situ generated MeOD solution of **3 +** remaining excess of Et_3N & $NaBH_4$, (c) b + 1atm CO_2 after 24 h and (d) b + 1atm CO_2 after 48 h .[1, 2, 5-7]

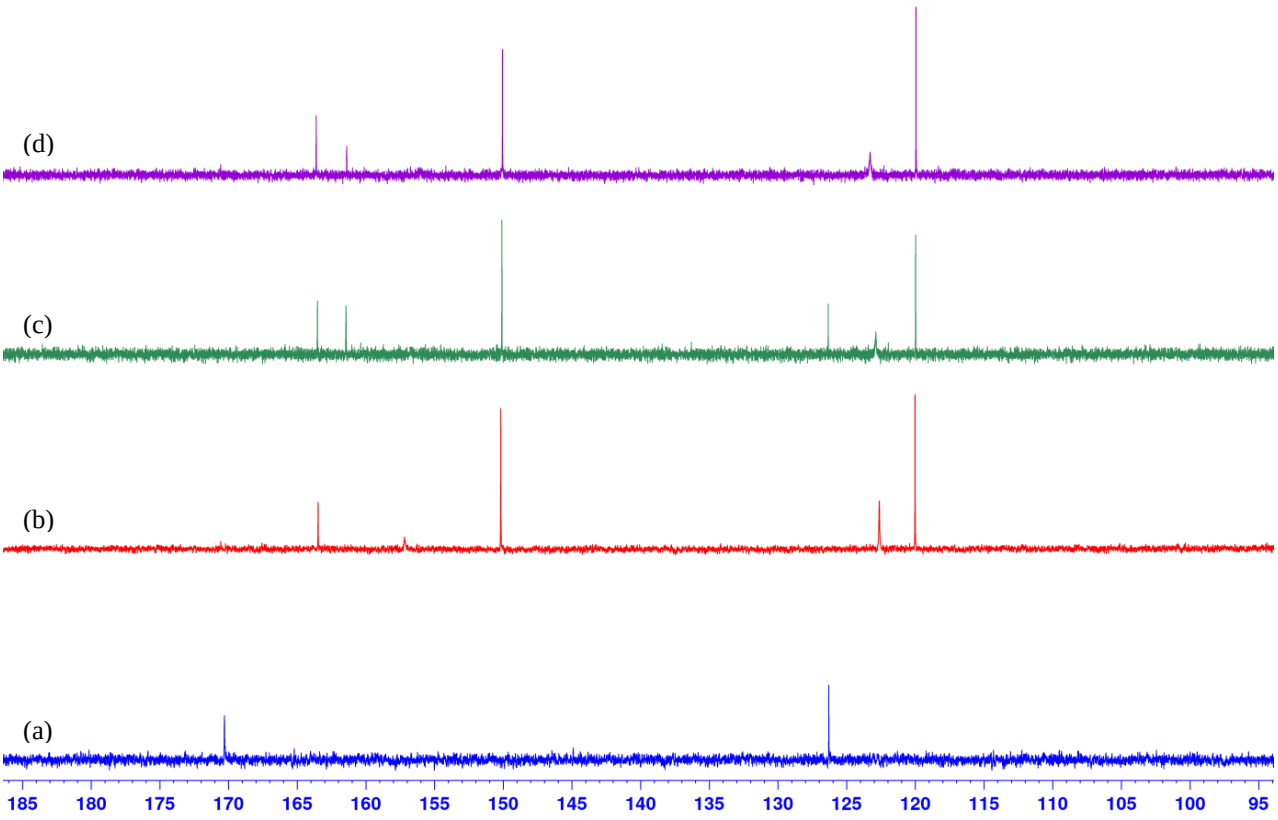

Figure S8. Magnified depiction of figure S7 of the range 95 ppm to 185 ppm, showing change in the structure over a period of 48 h.

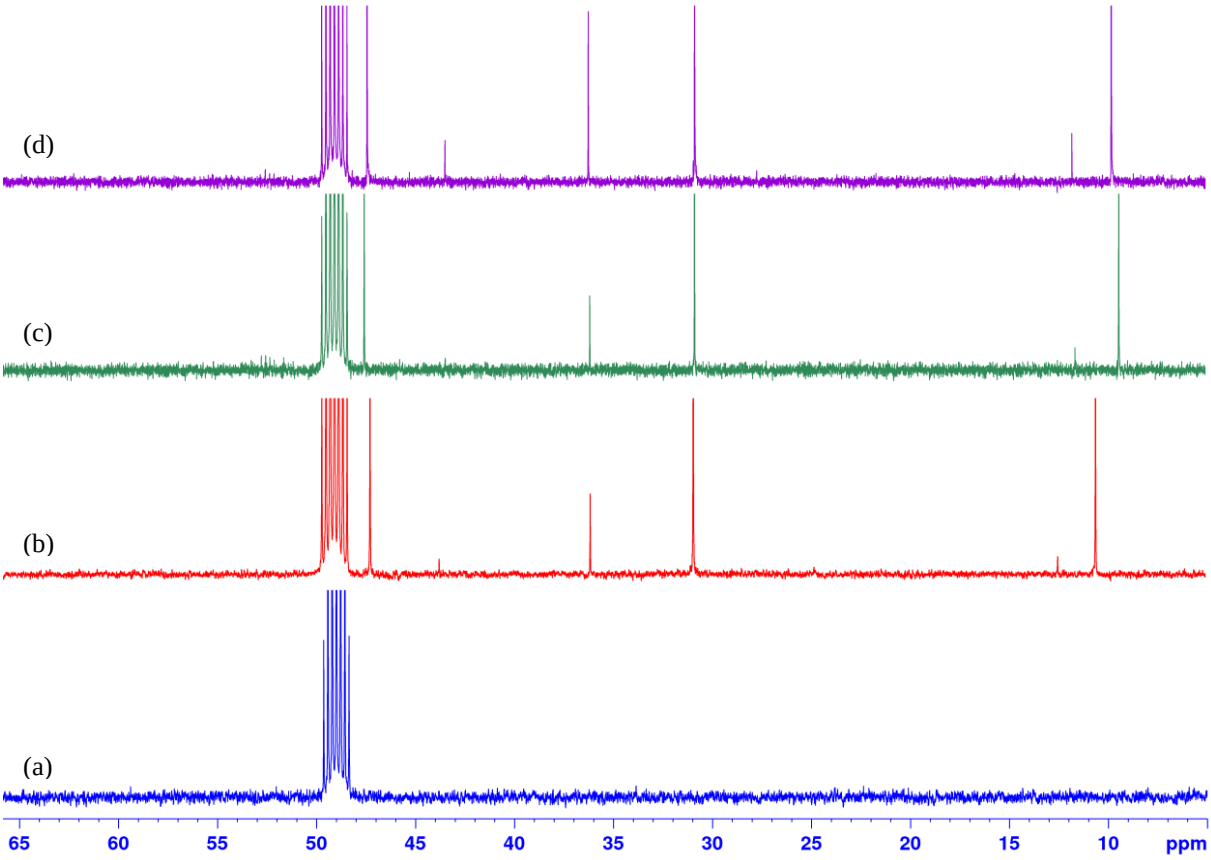

Figure S9. Magnified depiction of figure S7 of the range 5 ppm to 65 ppm, showing change in the structure over a period of 48 h.

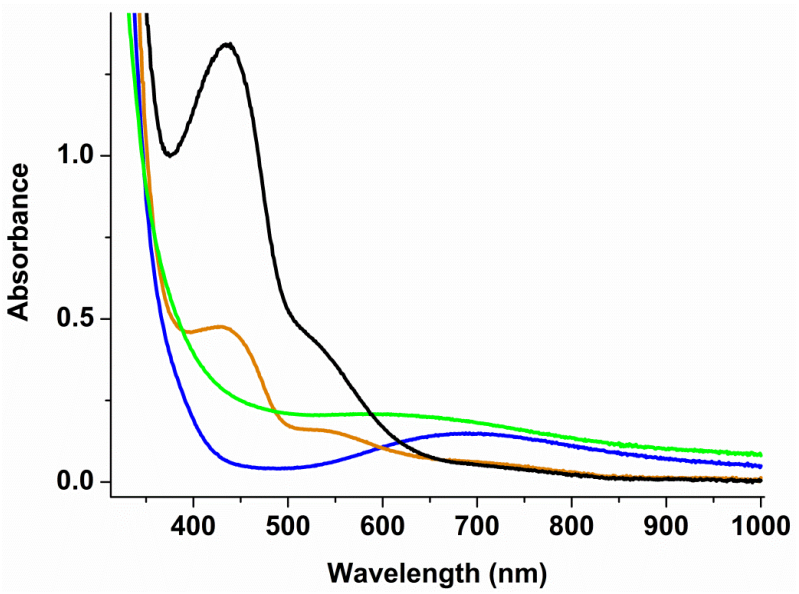

Figure S10. UV-Vis spectrums of 0.5 mM MeOD solution of **2** (blue trace), **3 +** air (after 1 minute, black trace), **3+** air (after 40 minute, brown trace) and **4** (green trace).

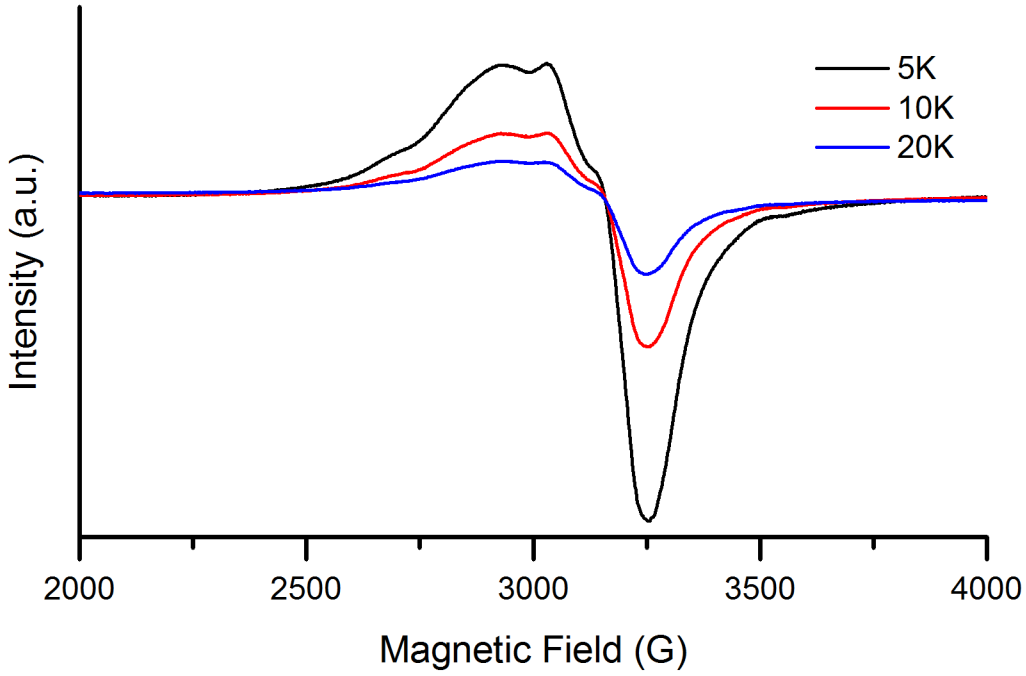

Figure S11. EPR spectra of **2** (1.3 mM in MeCN) at different temperatures, 5 K (black), 10 K (red) and 20 K (blue). EPR conditions: microwave power: 200 µW, microwave frequency 9.287 GHz.

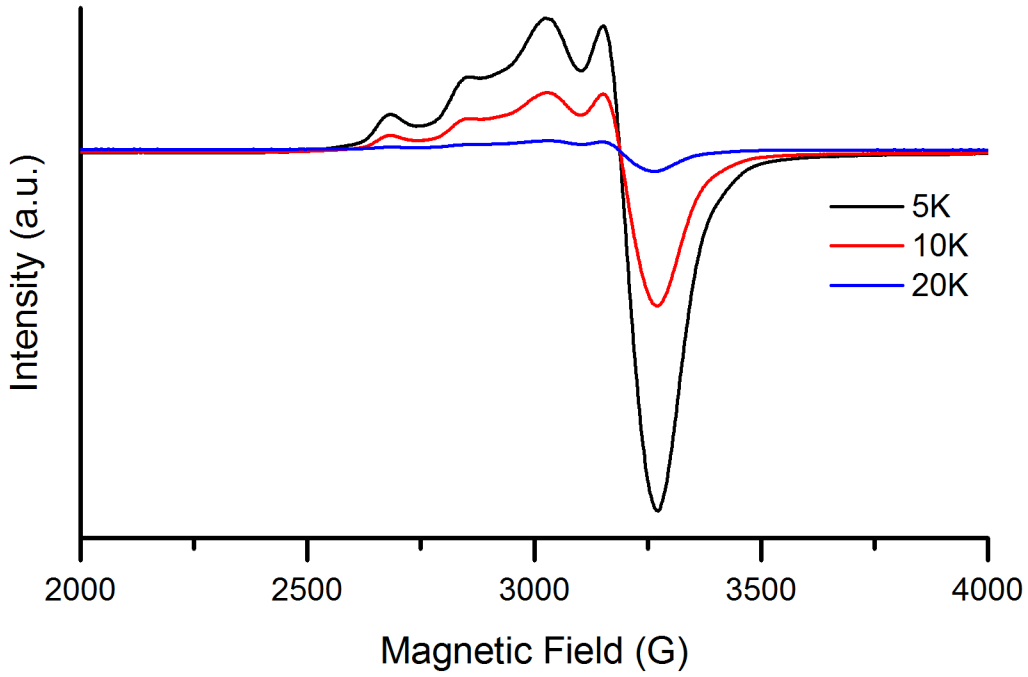

Figure S12. EPR spectra of **4** (1 mM in MeCN) at different temperatures, 5 K (black), 10 K (red) and 20 K (blue). EPR conditions: microwave power: 200 µW, microwave frequency 9.287 GHz.

1. C. V. Picasso, D. A. Safin, I. Dovgaliuk, F. Devred, D. Debecker, H.-W. Li, J. Proost and Y. Filinchuk, *International Journal of Hydrogen Energy*, 2016, **41**, 14377-14386.
2. I. Knopf and C. C. Cummins, *Organometallics*, 2015, **34**, 1601-1603.
3. C. Ziebart, C. Federsel, P. Anbarasan, R. Jackstell, W. Baumann, A. Spannenberg and M. Beller, *Journal of the American Chemical Society*, 2012, **134**, 20701-20704.
4. C. Federsel, C. Ziebart, R. Jackstell, W. Baumann and M. Beller, *Chemistry – A European Journal*, 2012, **18**, 72-75.
5. R. Zhang, Z. Liang, H. Liu, W. Rongwong, X. Luo, R. Idem and Q. Yang, *Industrial & Engineering Chemistry Research*, 2016, **55**, 3710-3717.
6. F. Mani, M. Peruzzini and P. Stoppioni, *Green Chemistry*, 2006, **8**, 995-1000.
7. G. R. Fulmer, A. J. M. Miller, N. H. Sherden, H. E. Gottlieb, A. Nudelman, B. M. Stoltz, J. E. Bercaw and K. I. Goldberg, *Organometallics*, 2010, **29**, 2176-2179.